EFFECT OF UNDERLYING SURFACE ON ACOUSTIC WAVE PROPAGATION NEAR THE GROUND

N.P. Krasnenko and L.G. Shamanaeva

Institute of Atmospheric Optics,
Siberian Branch of the Russian Academy of Sciences, Tomsk
Received December 30, 1994

A review of models of sound propagation near the ground through a homogeneous stationary atmosphere is presented. Existing models of acoustic impedance of the Earth's surface are analyzed.

Propagation of acoustic wave near the ground is affected by numerous factors among which are the impedance and the relief of underlying surface, the vertical profiles of the meteorological parameters, the atmospheric turbulence, and the directional pattern of an acoustic radiation source. At present, a unified theory of acoustic wave propagation allowing for combined effect of the above factors is lacking. In the literature we know (see, for example, Refs. 1–4 and 21) each factor is analyzed separately.

In this paper, a review of models of sound propagation near the ground on the material of foreign press is presented in which sound propagation through a homogeneous stationary atmosphere without constant gradients of the meteorological parameters is considered, and existing models of acoustic impedance of the Earth's surface are analyzed.

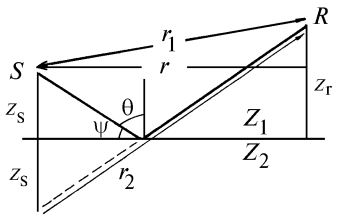

FIG. 1. Geometry of sound propagation near the ground. Here S denotes source and R denotes receiver of acoustic radiation.

Let acoustic radiation source be placed at altitude z_s above the Earth's surface, and a receiver be placed at a distance r from the source at altitude z_r. Then in addition to directly transmitted wave, the wave reflected from the underlying surface arrives at a receiving point, and the total acoustic pressure at this point can be written as[1]

$$P = P_\alpha + R_p P_r, \tag{1}$$

where P_α describes a contribution from directly transmitted wave, P_r describes a contribution from specularly reflected wave, and R_p is the wave reflection coefficient. For monochromatic radiation the phase difference between the directly transmitted and reflected waves is

$$\Delta\Phi = k\,(r_1 - r_2) + \Phi, \tag{2}$$

where Φ is the phase change after reflection from the underlying surface. When $\Delta\Phi = 180°$, the directly transmitted and reflected waves are in antiphase and produce an interference minimum. For *broadband acoustic signal*, its spectrum has minima at frequencies

$$f_m = c_0\,[(2n + 1)\,\pi - \Phi] \,/\, [2\,(r_2 - r_1)], \tag{3}$$

where c_0 is the sound speed in air. After reflection from a hard surface, $\Phi = 0$, while for free surface $\Phi = \pi$. In intermediate case of a porous surface $0 < \Phi < \pi$, and positions of minima in the received signal spectrum depend on the geometry of the experiment and the reflection coefficient of the underlying surface

$$R_p = |R_p|\, e^{i\Phi}, \tag{4}$$

which can be expressed as[2,3]

$$R_p = \frac{\sin\psi - (z_1 / z_2)\,\{1 - (k_1^2 / k_2^2)\cos\psi\}^{1/2}}{\sin\psi + (z_1 / z_2)\,\{1 - (k_1^2 / k_2^2)\cos\psi\}^{1/2}}. \tag{5}$$

Here ψ is the incidence angle, k_1 and k_2 are the wave numbers, z_1 and z_2 are the values of acoustic impedance of air and underlying surface, respectively, with $z_1 = \rho_0 c_0$, where ρ_0 is the density of air. For source and receiver altitudes small compared with the path length $\psi \to 0$, and Eq. (5) at glancing incidence angles has the form:

$$R_p = \sin\psi - \beta \,/\, \sin\psi + \beta\ , \tag{6}$$

where $\beta = 1/z = z_1/z_2$ is the surface conductivity.

For *spherical sound wave* both the directly transmitted and reflected waves undergo additional attenuation. In this case, the sound pressure level and the velocity of particles are expressed in terms of the acoustic velocity potential φ:

$$P = i\,\omega\,\rho_e\,\varphi, \qquad u = \frac{\partial\varphi}{\partial z}\ , \tag{7}$$

where $\omega = 2\pi f$; f is the sound frequency, in Hz; and ρ_e is the effective density of underlying surface. The velocity potential at the receiving point is[1]

0235-6880/95/10 827-06 $02.00

$$\varphi_r = \frac{\exp(i k_0 r_1)}{i k_0 r_1} + Q \frac{\exp(i k_0 r_2)}{i k_0 r_2}, \quad (8)$$

where $k_0 = \omega/c_0$ is the wave number in air, and Q is the spherical wave reflection coefficient. The acoustic potential reduced to a free space can be found from the relation

$$20 \log |\varphi_r / [e^{ik_0 r_1} / r_1]|. \quad (9)$$

When z_s and z_r are much greater than the propagation path length, the spherical wave reflection coefficient in Eq. (8) can be approximated by the plane wave reflection coefficient

$$Q = R_p, \quad (10)$$

where R_p is given by Eq. (6).

At glancing incidence angles $\psi < 5°$ for surface with high impedance, Q is approximated by the expression[1]

$$Q \approx R_p + (1 - R_p) F(W), \quad (11)$$

where $F(W)$ is the factor of boundary losses due to interaction of the incident spherical wavefront with the flat underlying surface given by the formula[1]

$$F(W) = 1 + i \sqrt{\pi W}\, e^{-W^2} \operatorname{erfc}(-i W). \quad (12)$$

Here $\operatorname{erfc}(-iW)$ is the error function, and W is the numerical distance given by the formula

$$W^2 = (1/2) (i k_0 r_2) (\beta + \cos\theta). \quad (13)$$

At incidence angles $\psi = 0$, from Eq. (6) we obtain $R_p = -1$. Equations (8) and (11) are then considerably simplified and

$$\varphi_r \approx 2 F(W) e^{ik_0 r}/r, \quad (14)$$

where, in accordance with Eq. (13)

$$W = (1/2) (1 + i) (k_0 r)^{1/2} \beta. \quad (15)$$

The second term in Eq. (11) is the correction for wavefront sphericity called the ground wave in analogy with the term employed in microwave region. For $|W| < 1$, that is, for high impedance and short path, from Eq. (12) we have

$$F(W) \approx 1 + i \sqrt{\pi}\, W e^{-W^2}. \quad (16)$$

For long path and low impedance ($|W| > 1$), we have

$$F(W) \approx 1 + i \sqrt{\pi}\, W e^{-W^2} H[-\operatorname{Im}(W)] - \frac{1}{2 W^2}, \quad (17)$$

where $H(x)$ is the Heaviside unit function, $H(x) = 1$ for $x \geq 0$ and $H(x) = 0$ for $x < 0$, and $\operatorname{Im}(W)$ denotes the imaginary part of the numerical distance W. The temporal dependence of received signal is assumed exponential. After substitution of Eqs. (16) and (17) in Eqs. (11) and (8), the following conclusions can be drawn. At glancing incidence angles, the acoustic pressure level from a point source in the near field is inversely proportional to the distance from the source, that is, decreases by 6 dB as the distance is doubled. In the far field, the sound pressure level is inversely proportional to the square of the distance, that is, decreases by 12 dB as the distance is doubled.

The Heaviside unit function in Eq. (17) significantly contributes for $r > 50$ m and $f < 300$ Hz in the case of sound propogation above the surface with low impedance, for example, above grass-covered ground. After substitution of this function in Eqs.(11) and (8) it engenders so-called surface wave, decreasing with the square root of the distance in the direction of propagation and exponentially with the altitude above the ground in the orthogonal direction. At glancing incidence angles, this function results in the increase of the imaginary part of impedance

$$Z = X + i Y, \quad (18)$$

that is, reactivity Y, which becomes greater than the real part of the impedance, or resistivity. The sharp action of the Heaviside unit function (its switching on and off) is due to approximation used in Ref. 1. More realistic asymptotic solutions to Eqs. (8), (12), and (13), known in the theory of propagation of electromagnetic waves as the Weyl-Van der Pol solutions were obtained in Refs. 5–8. However, comparison of these realistic solutions with results of calculations by formulas presented above made in Refs. 9 and 10 indicated their insignificant discrepancy.

The ground wave described by the second term in Eq. (11) is caused by incident spherical wavefront distortions due to interaction with flat underlying surface. The surface wave propagating near the boundary between two media is produced by elliptical motion of air molecules and their resultant motion parallel and perpendicular to a porous surface. The surface and ground waves transfer primarily the low-frequency acoustic radiation at long distances. In this case, the surface wave may increase the recorded sound pressure level, and its speed is slightly lower than the sound speed in air. This wave is observed at glancing incident angles above surfaces for which the imaginary part of impedance exceeds its real part. It should be noted that most surfaces exhibit high real impedance.

Propagation of sound wave from a *directional source* above the ground was studied in Ref. 11, where the acoustic potential of the source was represented as

$$\varphi_0 = \sum_{m=0}^{\infty} \sum_{n=-m}^{m} C_{nm} h_m^{(1)}(k r_0) P_m^{|n|}(\cos\theta) e^{in\Phi}, \quad (19)$$

where $h_m^{(1)}$ are the mth order spherical Hankel functions of the first kind, $P_m^{|n|}(\cos\theta)$ are the associated Lagendre polynomials, C_{nm} are the multiple moments which characterize the directional pattern of the source, and $\{r_0, \theta, \Phi\}$ are the spherical coordinates in the system whose origin is at $(0, 0, z_s)$.

For surfaces with $|W| \gg 1$, the received acoustic field is a sum of geometric and diffraction fields (or directly transmitted, ground, and surface waves). For

surface with pure imaginary conductivity $\beta = -i\beta_2$, where $\beta_2 > 0$, the acoustic potential can be written as

$$\varphi_r \mid -4\pi i\beta_2 e^{-k\beta_2(z+z_s)} \sum_{m=0}^{\$} \sum_{n=0}^{m} L_{nm} P_m^n(i\beta_2) \times$$

$$\times H_n^{(1)}(kr\sqrt{1+\beta_2^2}), \quad (20)$$

$$L_{nm} = D_{nm} e^{in\Phi} + (-1)^n D_{-nm} e^{-in\Phi}, \quad (21)$$

$$D_{nm} = (1/2)\, C_{nm} \exp(i\,\pi\,(n-m)\,/\,2), \quad (22)$$

$H_n^{(1)}$ is the nth order Hankel function of the first kind. Hence, the acoustic field above elastic surface with low losses is determined by the surface wave and attenuates as the square root of the distance.

For $|W| \lesssim 1$, that is, for moderate numerical distances, when $kr_2 \gg 1$ and $|(\beta^2 - \cos^2\theta)/\sin^2\theta| \ll 1$, the acoustic potential

$$\varphi_r \mid \varphi_0 + \sum_{m=0}^{\$} \sum_{n=-m}^{m} C_{nm} h_m^{(1)}(k\,r_2) P_m^{\ddot{o}n^{\ddot{o}}}(\cos\theta) R_p^{(\theta)} e^{in\Phi} -$$

$$- \frac{4}{ik} \frac{\beta F(\omega) \exp(ikr_2)}{(\cos\theta+\beta)\, r_2} \sum_{m=0}^{\$} \sum_{n=0}^{m} (-1)^n L_{nm} P_m^n(-\beta) \quad (23)$$

is the sum of geometric (the first and the second terms) and diffraction (the ground wave described by the third term) fields. When supplementary conditions

$$\cos\theta \ll |\beta| \text{ and } 2\,k\,(z\,z_s)\,/\,r_1 \ll 1$$

are satisfied, only the third term remains in Eq. (3), that is, sound field becomes pure diffraction one.

Comparison of Eqs. (20) and (23) with Eqs. (11), (16), and (17) indicates that the acoustic field of the directional source is not equal to the acoustic field of omnidirectional source multiplied by the directional pattern but depends nonlineary on the acoustic conductivity and the source directional pattern.

Effect of the underlying surface characteristics on propagation of a broadband acoustic signal is illustrated by an example of propagation of the jet engine noise shown in Fig. 2 borrowed from Ref. 1.

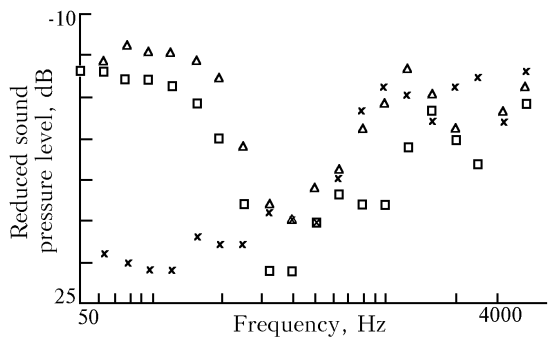

FIG. 2. Effect of the surface impedance for path of length of 347 m *in March (small triangles) and October (small crosses). Small squares are for snow–covered surface.*

Measurements were performed over a silt soil layer 1 m thick located above a layer of kaolin and over a rather thin fertile soil layer 5 cm thick located above a dense clay layer.

Both surfaces were covered with grass. The first run of measurements was performed in March and October, the second run of measurements – in winter. Measurement path was 347 m long. It can be seen from the figure that the first interference minimum over the snow cover whose thickness varied from 6 to 9 in. is deeper and occurs at much lower frequency than the first interference minimum over the grass–covered surface.

It is evident from the foregoing that the underlying surface affects the propagation of sound through the conductivity β. On the basis of the large quantity of experimental data Delany and Bazley[12] proposed the semiempirical formula for the acoustic impedance

$$Z = 1/\beta = 1 + 0.0571\, C_1^{-0.754} + i\ 0.087\, C_1^{-0.732}, \quad (24)$$

where $C_1 = \omega\rho_0/2\pi\sigma$, and σ is the flow resistivity.

In the range of acoustic frequencies, $0.01 < C_1 < 1$. The flow resistivity varies within the limits $10\,000 < \sigma < 20\,000\,000$ rayls (1 rayls = 1 N·cm^{-4}), and for grass–covered surface $\sigma \mid 300\,000$ rayls. However, Eq. (24) does not provide satisfactory agreement with experimental data. It seems likely that this is due to the use of the parameter C_1/Ω for normalization, where Ω is the porosity of a medium. For fibrous materials, $\Omega \approx 1$ and σ was determined experimentally. For soil, $\Omega \approx 0.5$ or even less. However, this model has received wide acceptance due to its simplicity. The values of σ for surfaces of different types are given in Refs. 3 and 13. It should be noted that with an increase in σ the amplitude of this minimum decreases and it is shifted toward higher frequencies. More correct prediction of sound propagation for single–parameter model (24) can be made based on preliminary measurements of the effective parameter σ_{eff} on a short path and its subsequent use for prediction of sound propagation at long distances.

The Sievel model[1] relates the frequency of interference minimum ω_m with the porosity Ω and the parameter of flow resistivity σ:

$$Z = \Omega\,(1 + i\,\Omega\sigma)\,/\,(\rho_0\,\omega)^{1/2}, \quad (25)$$

$$(\omega_0/\omega_m)^{1/2} = 0.906\,\lambda_m + 0.268/\lambda_m - 0.128/\lambda_m^3 +$$
$$+ 0.11/\lambda_m^5 + \ldots, \quad (26)$$

where $\lambda_m = 2\pi/f_m = \omega_m/C_0\sqrt{z_s z_r}$ and $\omega_0 = 2\pi f_0 = \sigma^2\Omega/\rho_0$. The experimental data shown in Fig. 2 are approximated by the Sievel model with $f_m = 400$ Hz. For $z_s = 1.8$ m and $z_r = 1.5$ m, this yields $f_0 = 6494$ Hz at $\Omega = 0.4$, hence, $\sigma = 122\,408$ rayls. In accordance with formulas (25) and (26), the parameter Z is independent of r. This conclusion was experimentally confirmed in Ref. 14.

However, formulas (24) and (25) do not explain different amplitudes of the interference minimum. This effect is allowed for the model of an absorbing layer of thickness d with acoustically hard backing whose impedance is

$$Z_1 = Z \cot(-i k_b d), \quad (27)$$

where Z is given by Eq. (24), and k_b is the complex wave number in porous medium which can be found from the relation[4]

$$k_b/k_0 = 1 + 0.0978\, C_1^{-0.693} + i\, 0.189\, C_1^{-0.618}. \quad (28)$$

Formula (27) describes the two-parameter model of the impedance. It was successfully used by Rasmussen[15] to interprete measurements over grass-covered surface.

A model of a porous layer above an acoustically harder surface can be recommended for forest underlying surface covered with snow or high vegetation:

$$Z = Z_1 [\{Z_2 - i Z_1 \tan(k_b d)\}/\{Z_1 - i Z_2 \tan(k_b d)\}], \quad (29)$$

where Z_1 is the characteristic impedance of the upper layer with the wave number k_b, and Z_2 is the characteristic impedance of the lower layer which is assumed semi-infinite. This model has three parameters. Results of calculations for the above model are shown in Fig. 3.

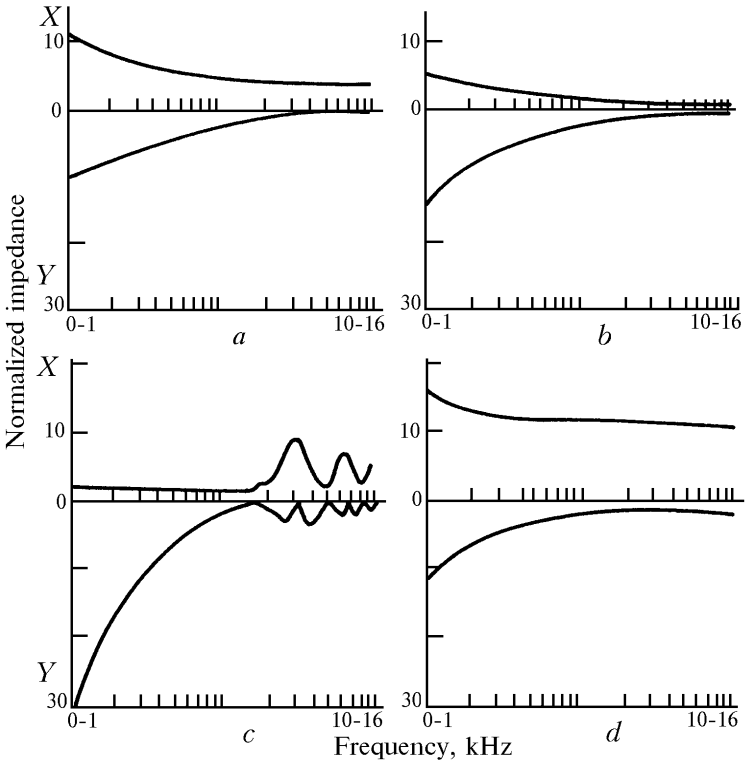

FIG. 3. Four models of surface impedance: a) single-parameter model, σ = 10 000 rayls; *b) model with variable porosity,* σ = 62 500 rayls, *and* α = 100 m^{-1} *(here* α *is the effective rate of decrease of porosity with increasing depth); c) a layer with hard backing,* σ = 160 000 rayls, Ω = 0.4, *and* d = 0.03 m; *d) multilayered model with* σ_1 = 100 000 rayls, Ω_1 = 0.4, d_1 = 0.03 m, σ_2 = 300 000 rayls, *and* Ω_2 = 0.2.

Experimental study of the impedance of underlying surfaces of different types was performed in Refs. 19, 22, and 23. Figure 4 shows the normalized impedance of a layer of sand 4.1 cm thick above a hard backing measured in Ref. 22 by the technique proposed in Ref. 23 which incorporates sound pressure level measurements at different distances from the source (loudspeaker with a conic horn with an aperture of 16 cm located at an altitude of 15 cm above the ground) along two horizontal paths located at altitudes of 2.2 and 4.6 cm above the ground. Maximum measuring path length was 1.75 m, measurements were taken at 1 cm intervals.

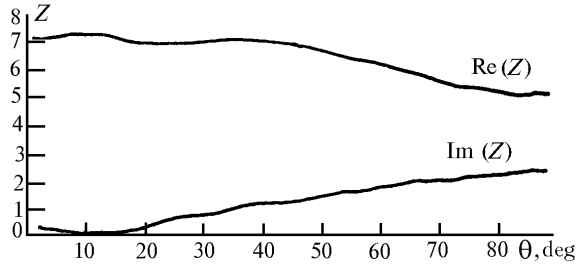

FIG. 4. Experimental dependence of the normalized impedance of sandy surface on the angle of wave incidence borrowed from Ref. 22. Sound frequency is 1000 Hz.

Effect of porous surface is illustrated by Fig. 5. Here the reduced sound pressure level measured above a porous pavement (dashed stone, $\Omega = 30\%$) and a hard asphalt cover is shown. It should be noted that an increase in the sound pressure level above the porous surface is caused by the surface wave which is amplified above the porous surface.[22]

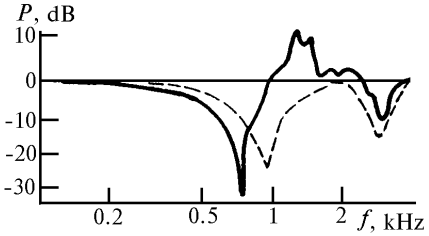

FIG. 5. Experimental frequency dependence of the reduced sound pressure level above porous (solid curve) and hard (dashed curve) surfaces, $z_s = z_r = 0.6$ m, *and* $r = 4$ m.

Below we present some simple models proposed by Attenborough[16] on the basis of formulas (25)–(29) and recommended for concrete types of the Earth's underlying surfaces.

1. Sand and hard soil without vegetation

$$Z = 0.218\,(\sigma/f)^{1/2}\,(1 + i). \qquad (30)$$

2. Grass cover

$$Z = 0.218\,(\sigma/f)^{1/2} + i\,[0.218\,(\sigma/f)^{1/2} + 9.74\,(\alpha/f)], \qquad (31)$$

where α is the effective rate of decrease of porosity Ω with increasing depth. Exponential decrease of porosity is assumed.

3. Forest cover

$$Z = 0.000\,82\,\sigma\,d + i\,(38.99/(f/d)), \qquad (32)$$

where d is the effective thickness of a layer with hard backing.

For model (31), the reactivity is greater than the resistivity, $Y > X$, and the frequency dependence is stronger. For a thin-layer model described by Eq. (32), X is independent of f, and $Y \mid 1/f$.

In conclusion, the four-parameter model proposed by Thomasson[17] should be mentioned, which includes, in addition to the parameters σ and Ω, the parameter of pore slope describing the angle of deflection of the air pore sense from the direction orthogonal to the layer boundary and the form factor describing a degree of deviation of a typical pore shape from circular cylinder, for which it is equal to 0.5. However, this model has not yet found widespread use due to the complexity of determination of its parameters.

It also should be noted that all types of underlying surfaces under study exhibited local reaction, that is, the reflected wave, the incident wave, and the normal at the point of incidence all lay in the same plane, and the acoustic surface impedance was assumed independent of the incidence angle. Surfaces with low flow resistivity, for example, a layer of snow above a porous fertile soil layer ($\sigma \mid 30\,000$ rayls), exhibits extended reaction. Results of experimental investigations of underlying surfaces of extended reaction were presented in Refs. 18 and 19. For surface of extended reaction, the spherical wave reflection coefficient Q is given by Eq. (11), like in the case of surface of local reaction, the factor of boundary losses $F(W)$ is given by formula (12), and the numerical distance is approximated by expression[19]

$$W = 2ik_1r_2\kappa(k_1, k_2, \psi)\,(1/Z)^2/[(1-R_p)^2\cos^2\psi], \qquad (33)$$

where

$$\kappa(k_1, k_2, \psi) = 1 - k_1^2 / k_2^2\cos^2\psi\,, \qquad (34)$$

and R_p is the plane wave reflection coefficient given by the formula

$$R_p = \frac{Z\sin\psi - [\kappa(k_1, k_2, \psi)]^{1/2}}{Z\sin\psi + [\kappa(k_1, k_2, \psi)]^{1/2}}\,. \qquad (35)$$

The model adequately describes the sound pressure level in the case of sound propagation above the surface of extended reaction.

The effect of the underlying surface relief is treated by the ray tracing technique for the given geometry of the surface. In so doing, the reflection coefficient is determined from Eq. (11). A simple method for calculation of sound attenuation by a rectangular barrier located between the source and the receiver was proposed in the Draft International Standard.[24] By this method, the sound pressure level at the receiving point is calculated as a sum of contributions of waves emitted by the source and propagating along three shortest path, one of which passes through the barrier top and two others through the barrier sides. A thick barrier is substituted by an equivalent thin barrier[25] placed at the intersection of rays coming from the source and the receiver and passing through the corresponding sides of the barrier.

To evaluate numerically excess attenuation of sound by reflectors of finite dimensions (for example, by walls of buildings, barriers, and so on) and by semi-infinite screens, the methods of the diffraction theory are used (see Refs. 26 and 27).

The effect of surface relief was studied in Refs. 20, 25, and 28. A model experiment on acoustic propagation over countered grass-covered surface with finite impedance and $\sigma = 300\,000$ rayls was performed by Hitchins et al.[20] Measuring path was 50 m long. The underlying surface was inclined, wavy, or hilly. Figure 6 shows measurements on the path with a hill between the source and the receiver. The hill shape was sinusoidal. Additional minimum is seen in the figure for

the source located near the ground. It is also seen that the underlying surface relief has a marked effect on sound wave attenuation, engendering additional interference minima. It must be taken into account when making prediction of sound wave propagation.

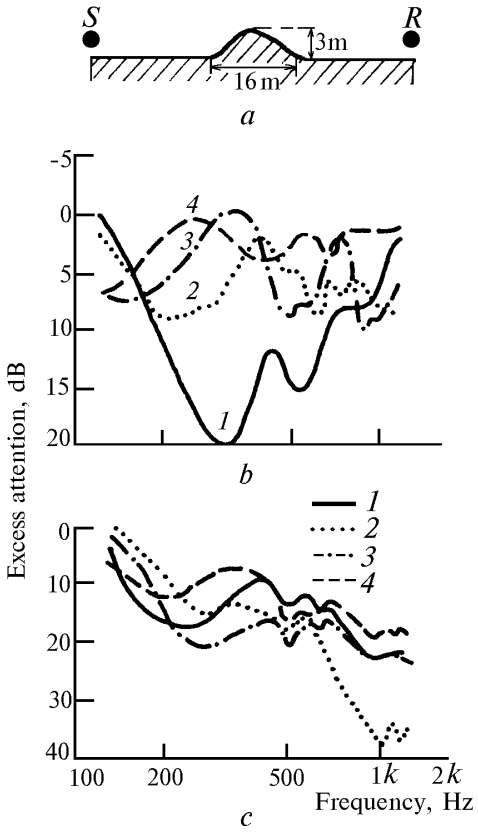

FIG. 6. Effect of countered surface: a) path with a hill, r = 50 m; *b) excess attenuation for* $z_s = z_r = 1(1)$, $2(2)$, $3(3)$, *and* 4 m(*4*); c) excess attenuation for $z_s = 0$ *and* $z_r = 0(1)$, $1(2)$, $2(3)$, *and* 3 m(*4*).

REFERENCES

1. K.A. Attenborough, Appl. Acoust. **24**, 289 (1988).
2. D.A. Bohlender, F. Babott, P.J. Irwin, and T. Mathews, J. Sound Vib. **105**, No. 2, 283 (1986).
3. N.N. Bochkarev and N.P. Krasnenko, "*Peculiarities of sound wave propagation near the ground*,B Preprint, No. 501—B—86, VINITI Moscow (1985).
4. M.E. Delany and E.N. Bazley, J. Sound Vib. **13**, 269 (1970).
5. D. Habault, J. Sound Vib. **79**, 551 (1981).
6. P.J.T. Filippi, J. Sound Vib. **91**, 65 (1989).
7. S.T.I. Thomasson, Acustica **45**, 122 (1980).
8. M. Nobile and S.I. Hayek, J. Acoust. Soc. Am. **78**, 1325 (1985).
9. L.R. Quartazaro, "*A theoretical investigation of sound propagation above a half—space of extended reaction*,B MS Thesis, Pensylvania State University (1983).
10. K. Attenborough, N.W. Heap, T.L. Richards, and V.S. Sastry, J. Sound Vib. **84**, 289 (1982).
11. A.V. Generalov, Akust. Zh. **33**, No. 6, 998 (1987).
12. M.E. Delany and E.N. Bazley, Appl. Acoust. **3**, 105 (1970).
13. T.F.W. Embleton, J.E. Piercy, and G.A. Daigle, J. Acoust. Soc. Am. **74**, 1239 (1984).
14. P.H. Parkin and W.E. Scholes, J. Sound Vib. **2**, 353 (1965).
15. K.B. Rasmussen, J. Sound Vib. **78**, 247 (1981).
16. K. Attenborough, in: *Inter—Noise 84*, Honolulu, USA (1984), p. 295.
17. S.I. Thomasson, J. Acoust. Soc. Am. **61**, 659 (1977).
18. J. Nicolas, J.L. Berry, and G.A. Daigle, J. Acoust. Soc. Am. **77**, 67 (1985).
19. M.C. Berengier, in: *Inter—Noise 93*, Leuven, Belgium (1993), p. 513.
20. D.A. Hutchins, H.W. Jones, and L.T. Russel, Acustica **58**, 235 (1985).
21. N.G. Abramov, A.Ya. Bogushevich, V.I. Karpov, N.P. Krasnenko, and A.A. Fomichev, Atmos. Oceanic Opt. **7**, No. 3, 215 (1994).
22. C. Verhaegen, W. Lauriks, and A. Corps, in: *Inter—Noise 93*, Leuven, Belgium (1993), p. 519.
23. C. Verhaegen, W. Lauriks, and A. Corps, in: *Proceedings of the Fifth International Symposium on Long—Range Sound Propagation,* Milton Keynes, U.K. (1992), p. 1.
24. ISO/DIS 9613—2: *Attenuation of Sound During Propagation Outdoors.* Part 2. *A General Method of Calculation,* Draft International Standard ISO (1992).
25. Y.W. Lam and R.M. Windle, in: *Inter-Noise 93*, Leuven, Belgium (1993), p.501.
26. A.E. Charles and D.M. Allen-Booth, in: *Inter-Noise 93*, Leuven, Belgium (1993), p. 1727.
27. K. Yamamoto and K. Takagi, Appl. Acoust., No. 37, 75 (1992).
28. K. Yamamoto, R. Hotta, and K. Takagi, in: *Inter-Noise 93*, Leuven, Belgium (1993), p. 1739.